Nuclear Engineering and Design 441 (2025) 114183

Contents lists available at ScienceDirect

Nuclear Engineering and Design

journal homepage: www.elsevier.com/locate/nucengdes

High-fidelity and high-resolution simulation of two different rod ejection accidents in a NuScale-like small modular reactor with conventional and accident tolerant fuels

Zsolt Soti [a,*], Paul Van Uffelen [a], Arndt Schubert [a], Ville Valtavirta [b], Riku Tuominen [b], Heikki Suikkanen [c], Ville Rintala [c], Andre Gommlich [d], Emil Fridman [d], Yurii Bilodid [d], Luigi Mercatali [e], Victor Hugo Sanchez-Espinoza [e]

[a] European Commission, Joint Research Centre Karlsruhe, Germany
[b] VTT Technical Research Centre of Finland, Finland
[c] Lappeenranta-Lahti University of Technology LUT, Finland
[d] Helmoltz-Zentrum Dresden-Rossendorf, Germany
[e] Karlsruhe Institute of Technology, Germany

A B S T R A C T

This work presents a high-fidelity pin-by-pin simulation approach for a NuScale-like Small Modular Reactor core during a rod ejection accident (REA). We coupled 3D Monte Carlo neutron transport (Serpent), subchannel thermal–hydraulic (SUBCHANFLOW) and fuel performance (TRANSURANUS) codes using the Interface for Code Coupling (ICoCo), which is part of the EU's Salome open source platform. To resolve fuel intra-assembly details, we simulated all the fuel rods and channels, subdividing them into axial slices and transferred calculated data between the codes using scalar fields saved in memory variables. Two different REA scenarios were modelled, and the behaviour of fresh-loaded cores with conventional UO_2 fuel with Zr-4 cladding and accident tolerant fuel (ATF) materials, U_3Si_2 fuel with FeCrAl cladding, were analysed. In both scenarios, the control rod was ejected within 0.1 s, followed by a SCRAM after two seconds. In the first moderate scenario, the control rod ejection occurred at 75% of the nominal power, whereas in the second accident scenario, it occurred at hot zero power (HZP) conditions. In the first scenario, the power increase was around 25%, while in the HZP case it amounted up to 600% and 300% of the nominal power for the core loaded with UO_2 and ATF-fuel and cladding, respectively. Detailed calculations were conducted on a High-Performance Computer (HPC). The results demonstrated the robustness and flexibility of the coupled code system, providing full-core behaviour and rod-level safety parameters and predicting as needed during the safety analysis support of the licensing processes. This paper outlines the system setup, presents rod-level results and underlines the usefulness to assess the performance of SMR-cores loaded with different fuel types under various REA scenarios. In the scenarios considered, we did not observe significant fuel rod deformations, and the core loaded with ATF-fuel and cladding showed a large margin to melting.

1. Introduction

Small Modular Reactors (SMRs) are being considered to reduce the carbon footprint of the energy production sector (electricity, heat, etc.). There are many SMR-designs, some of them under construction, others under review by regulators. In a similar way as for larger nuclear reactors, their safety analyses must be carried out with due regard to the reduced core size and several other design differences. Unfortunately, there is still a limited amount of experimental data of safety-relevant phenomena available for the validation of the numerical tools to be used for the safety analysis of SMRs in the frame of licensing.

Traditional safety analyses couple nodal diffusion codes, such as PARCS, with thermal–hydraulic (TH) codes. However, these methods are limited in their ability to directly predict local safety parameters. For example, they cannot determine the precise location of the hottest or coldest fuel pin within the core. The pin power is approximated and transferred to a standalone subchannel code for TH simulation without incorporating any feedback between neutronics (N) and TH.

To increase the details in the simulation and reduce the level of approximations, high-fidelity Monte Carlo (MC) neutronics codes like

* Corresponding author.
E-mail addresses: Zsolt.Soti@ec.europa.eu (Z. Soti), Paul.VAN-UFFELEN@ec.europa.eu (P.V. Uffelen), Arndt.Schubert@ec.europa.eu (A. Schubert), Ville.Valtavirta@vtt.fi (V. Valtavirta), Riku.Tuominen@vtt.fi (R. Tuominen), heikki.suikkanen@lut.fi (H. Suikkanen), Ville.Rintala@lut.fi (V. Rintala), a.gommlich@hzdr.de (A. Gommlich), e.fridman@hzdr.de (E. Fridman), y.bilodid@hzdr.de (Y. Bilodid), luigi.mercatali@kit.edu (L. Mercatali), victor.sanchez@kit.edu (V.H. Sanchez-Espinoza).

https://doi.org/10.1016/j.nucengdes.2025.114183
Received 17 January 2025; Received in revised form 14 April 2025; Accepted 23 May 2025
Available online 30 May 2025

Serpent2 can be integrated into the coupling scheme. Moreover, including thermo-mechanical (TM) fuel performance codes such as TRANSURANUS enables detailed modelling of irradiation effects in the fuel pellet, gap and cladding of each individual pin. This approach provides a more realistic and physically consistent prediction of key parameters such as fuel material composition, the gap heat transfer coefficient, and cladding deformation variations along the height of the fuel rod. The interdependencies and feedback between codes can be realised through standardised data exchange mechanisms during the coupled simulations.

To address both the lack of experimental data and the need for accurate behavioural prediction in light water SMRs, the H2020 Euratom project McSAFER (Sanchez-Espinoza, 2021) was carried out. Its main objective was to advance the safety research for SMRs by combining safety-relevant thermal–hydraulic experiments with advanced numerical simulations at different spatial resolution levels. During the McSAFER project, valuable experimental data for the validation of advanced thermal–hydraulic simulation tools were obtained. In parallel to this, different N/TH/TM coupling schemes have been developed with the main goal to be able to perform pin-by-pin and subchannel-by-subchannel reactor core modelling.

This paper presents a beyond-state-of-the-art, high-fidelity multi-physics simulation approach that couples Serpent2 (N) SUBCHANFLOW (TH) and TRANURANUS (TM) codes. The framework includes detailed geometry, material properties and energy distributions and accounts for local feedback between the codes. This allows for the prediction of safety parameters at the local level and provides very accurate reference data about the behaviour of SMR cores. The presented high-fidelity simulation approach is characterised by fine time and spatial resolution focusing on individual pins and subchannels rather than entire fuel assemblies. The interaction of neutrons with matter is modelled without approximations regarding the angle and energy dependency of the interactions. To illustrate the capabilities of the coupling, we analyse reactor core behaviour during rod ejection accident (REA) scenarios applying them to conventional fuel and accident tolerant or sometimes referred to as advanced technology fuels (ATF). These simulations represent valuable tools for safety analysis and can provide support to the licensing process for most of the current advanced small reactor designs.

In the recent past, several papers have dealt with similar tasks. As far as the N/TH coupling is concerned, a REA scenario occurring in a SMART-like core has been investigated at different resolution levels by KIT (Mercatali et al., 2023). In this study, the authors compared the coupling of the PARCS/SUBCHANFLOW with Serpent2/SUBCHANFLOW REA simulations. The PARCS nodal approach was verified against the high-fidelity Monte Carlo based approach represented by Serpent2. Moreover, VTT colleagues carried out multi-physics coupling of fast transients in VVER-1000 and VVER-440 reactor cores by means of Serpent2/FINIX and HEXTRAN/FINIX coupled codes, respectively (Ikonen, 2016). The FINIX code is primarily designed as a transient simulation code compared to full-fledged fuel performance codes such as FRAPTRAN and TRANSURANUS and was not ready for ATF materials.

Xu et al (Xu, 2022) performed N/TH/TM coupling for conventional LWRs and also made a preliminary analysis of some ATF during normal operation conditions. The linear heat rate obtained from the NECP-X neutronics code was provided to the thermal-hydraulics CTF code, whereas CTF actually would need the clad heat flux rather than the pellet fission power during transients like the REA considered in this work. In this coupling, the NECP-CALF represented the TM code. Zahur et al (Zahur et al., 2023) also analysed the coupling of RAST-K/CTF/FRAPCON codes for the multicycle depletion analysis, i.e. not considering transients. They showed the benefits from two-way coupling between fuel performance and thermal–hydraulic codes in terms of more accurate and reliable analysis of safety parameters, such as the pellet centreline temperature during normal operation. Numerous research groups worldwide have undertaken the development of coupled simulation schemes. Table 1 provides a comparative overview of the aforementioned codes and methodologies.

More recently, based on the publicly available reference data, HZDR and VTT defined and analysed the neutronics benchmark of the NuScale-like core in the frame of the McSAFER project (Fridman et al., 2023). In this paper, we build on this experience and coupled three advanced tools to perform the intra-assembly and intra-rod modelling of the interdependencies of the neutronic, the fuel thermo-mechanics, and the coolant thermo-hydraulic behaviour during core transients. In future work, we intend to extend the presented simulations to other rector types, such as SMART. The similarities and differences between the NuScale and SMART designs are summarised in Table 2.

It is important to note that while MC neutronics methods offer high-fidelity results, they are time consuming. To address this, Serpent2 supports intensive parallelisation, which can be efficiently executed on modern High Performance Computer (HPC) systems that offer multiple computational nodes and numerous CPUs for parallel processing. Recent studies demonstrated that significant speedups in computationally intensive transient core simulations could be realized by leveraging GPU architectures. To utilise the massive parallelisation capabilities of GPUs in time dependent core simulations, instead of the traditional generation-by-generation neutron tracking approach the MC codes should apply the time-step method, as recommended by Molnar B et al. (Molnar et al., 2019).

The modular architecture of the presented ICoCo coupling framework, with standardised MEDCoupling interfaces for data exchange, provides a future pathway to substitute the coupled MC kernel with GPU-enabled versions for further reducing simulation time.

The Serpent2 Monte Carlo neutron transport (Leppänen, 2015), SUBCHANFLOW subchannel thermal–hydraulic (Imke and Sanchez-Espinoza, 2012) and TRANSURANUS fuel performance codes (Lassmann, 1992; Van Uffelen et al., 2007) were earlier successfully validated for conventional reactor modelling. The coupling made use of the Interface for Code Coupling (ICoCo) (Deville and Perdu, 2021), which is part of the European Salome platform. The ICoCo approach applies the object-oriented design and the mesh-based data transfer between the codes. The initial ICoCo code coupling for steady-state and depletion calculations of current PWRs loaded with conventional nuclear fuel was developed in the frame of the previous McSAFE project (Sanchez-Espinoza, 2021; García, 2020; García, 2021). In this paper, we present the system extensions, developed in McSAFER project, to model SMRs under transient conditions with conventional (UO_2) and ATF. For that purpose, the new SMR's core geometry, the material properties and correlations for uranium disilicide (U_3Si_2) fuel with FeCrAl cladding (ATF) are introduced. Additionally, we modelled the transient power transfer for the REA event. Because in transient scenarios, the power transfer from a fuel rod to the coolant is slower than the power generation in the same rod, the energy accumulation in the rod must be modelled in detail along with all its consequences by means of the TRANSURANUS code of the JRC.

The selected ATF has been extensively studied in (Chen and Yuan, 2017), demonstrating several advantages over conventional fuel, such as excellent oxidation resistance and the potential for reduced uranium enrichment. However, one significant disadvantage of this fuel/cladding combination is the larger thermal neutron cross section of the FeCrAl cladding. In (Zhang, 2021) the authors simulated the performance of the U_3Si_2 – FeCrAl system in a small reactor and found a significant neutron economy penalty, along with negative feedback on reactivity compared to conventional fuel designs.

The following sections present the detailed setup and the results of our SMR REA simulations with conventional fuel and ATF:

- The second section describes the modelled light water cooled NuScale-like SMR core. Since the reactor concept is a commercial product, not all relevant information is public; therefore, the reactor core setup was developed based on the currently available open

Table 1
Some coupling schemes of different N, TH and TM codes. The last line represents the research presented in this paper.

Codes	Coupling scheme	Power generation	Reactor type	Material	Operational conditions
PARCS/SCF	N/TH	deterministic	SMR	conventional	transient
Serpent2/SCF	N/TH	Monte Carlo	SMR	conventional	transient
Serpent2/FINIX	N/TM	Monte Carlo	conventional	conventional	transient
HEXTRAN/FINIX	N/TM	deterministic	conventional	conventional	transient
NECP-X/CTF/NECP-CALF	N/TH/TM	Monte Carlo	conventional	ATF	normal
RAST-K /CTF/FRAPCON	N/TH/TM	deterministic	conventional	conventional	normal
Serpent2/SCF/TRANSURANUS	N/TH/TM	Monte Carlo	conventional	conventional	normal
Serpent2/SCF/TRANSURANUS (presented in this study)	N/TH/TM	Monte Carlo	SMR	ATF & conventional	transient

Table 2
Similarities and differences between NuScale and SMART like SMRs.

Feature	NuScale design	SMART design
Reactor type	Integral PWR	Integral PWR
Thermal power	160 MWt	330 MWt
Coolant & moderator	Light water	Light water
Cooling mechanism	Natural circulation (no coolant pumps)	Coolant pumps used
Reactivity control	Soluble boron & control rods	Soluble boron & control rods
Core assemblies	17 × 17	17 × 17

literature. The missing data necessary for modelling was determined based on the expert judgements. Since our work primarily aimed to create, describe, demonstrate and discuss a coupling method for SMRs, the use of some nominal values does not affect the conclusions.

- In the third section, the various codes as well as the coupling methodology are outlined.
- The fourth section describes the modelling scenarios starting from the benchmark of VTT and HZDR (Fridman et al., 2023). Two REA scenarios are set-up for two different freshly loaded fuel types. Both REA scenarios occurred after 48 h of reactor run in a steady state. The scenarios were applied to conventional UO_2 and $UO_2 + Gd_2O_3$ fuel with Zr-4 cladding and to ATF, U_3Si_2 fuel with FeCrAl cladding. The same core geometry is used in both scenarios.
- Section five presents and discusses the results of the detailed high-fidelity and high time and spatial resolution intra-fuel modelling of the transient behaviour of the SMR with conventional fuel and ATF.
- In the sixth section, conclusions about the coupled simulation are drawn.
- Finally, perspectives are outlined in the seventh section.

2. NuScale-like core description

A detailed description of the NuScale-like core was taken from (Fridman et al., 2023). The commercial concept of the NuScale reactor design was developed by NuScale Power LLC. The U.S. Nuclear Regulatory Commission has certified the concept (US NRC, 2022). It is a pressurised water reactor (PWR) design, where the pressuriser and steam generators are housed within a compact vessel. The primary coolant system operates without pumps, utilising natural circulation to drive the coolant flow. The maximum power output considered in this manuscript is 160 MWth or 50 MWe.

The core specifications used in this modelling study are derived from the public version of the Final Safety Analysis Report (FSAR) submitted to the U.S. Nuclear Regulatory Commission (NRC) (L.L.C. NuScale Power, 2020). While the report does not provide all critical design parameters, some aspects important for modelling, such as the equilibrium core loading with fresh fuel of variable U-235 enrichment and the positioning of control rods, were determined based on expert judgment. Additionally, a simplification was made for the radial heavy reflector design.

The core contains 37 assemblies grouped in seven categories based on U-235 enrichment. The core loading with conventional fuel rods is shown on the left side of Fig. 1. Four fuel assemblies of type C02 contain 16 Gd_2O_3 pins. The right side of Fig. 1 shows the positions of 16 control rod assemblies (CRA), with regulation (RE) and shutdown (SH) banks. The core is surrounded by a heavy steel reflector and enclosed by a cylindrical core barrel, which are also depicted in Fig. 1. Further dimensions include 21.5036 cm for assembly pitches, 1.2598 cm for rod pitches. The radius of a fuel pellet is 0.4058 cm with a cladding outer radius of 0.4750 cm. The axial length of the fuel rod is 224.381 cm. The coolant is H_2O with 1000 ppm boron. Fig. 2 shows the two different fuel assembly layouts.

The core behaviour during rod ejection transient conditions was simulated for two different fuel types: conventional (UO_2) and ATF. The loading pattern in both cases is very similar except for the enrichment of the fuel rods. Conventional fuel pellets consist of UO_2 or $UO_2 + Gd_2O_3$ materials and Zr-4 cladding, as shown in Figs. 1 and 2. A detailed material description of control rods and other fuel materials is provided in (Fridman et al., 2023). ATF pellets consist of U_3Si_2, with cladding material made of FeCrAl. All fuel and cladding properties were inferred from data and correlations found in the open literature (cf. below).

3. Description of the coupled codes and coupling methodology

To achieve high-resolution, pin-by-pin, full core transient modelling of the SMR, three codes were coupled that have a strong background in conventional reactor modelling: Serpent2 (SSS), SUBCHANFLOW (SCF), and TRANSURANUS (TU). In the earlier McSAFE project (Sanchez-Espinoza, 2021), these codes were extended with ICoCo methods to perform steady-state and burnup modelling of conventional PWRs (García, 2020). The ICoCo extensions have enabled communication with a supervisor program and exchange calculated scalar fields via shared memory variables. The MED library classes and methods from the Salome platform (Salome Platform, 2018; MED Module and Documentation, 2018) were employed to manipulate and transfer these fields between the codes. Within the coupled SSS-SCF-TU system, all three codes and the extensions were compiled as shared object files.

During this new development phase in the frame of McSAFER project, we prepared input files tailored for the NuScale-like SMR, incorporated the material properties of ATF, and modified the ICoCo interfaces to be able to simulate transient behaviour during a rod ejection accident (REA). The subsequent paragraphs provide a brief overview of the three coupled codes and the coupling methodology. For further details, the reader is referred to the literature cited in the references.

3.1. Serpent2

Serpent2 (denoted as SSS) is a 3D continuous-energy Monte Carlo neutron and photon transport code developed at the VTT Technical Research Centre in Finland (Leppänen, 2015). In this coupling approach, the Serpent 2.1.32 version, which had been equipped with the ICoCo interface, was used. SSS code can perform various calculations, including reactor core steady-state, depletion and transient analyses. It

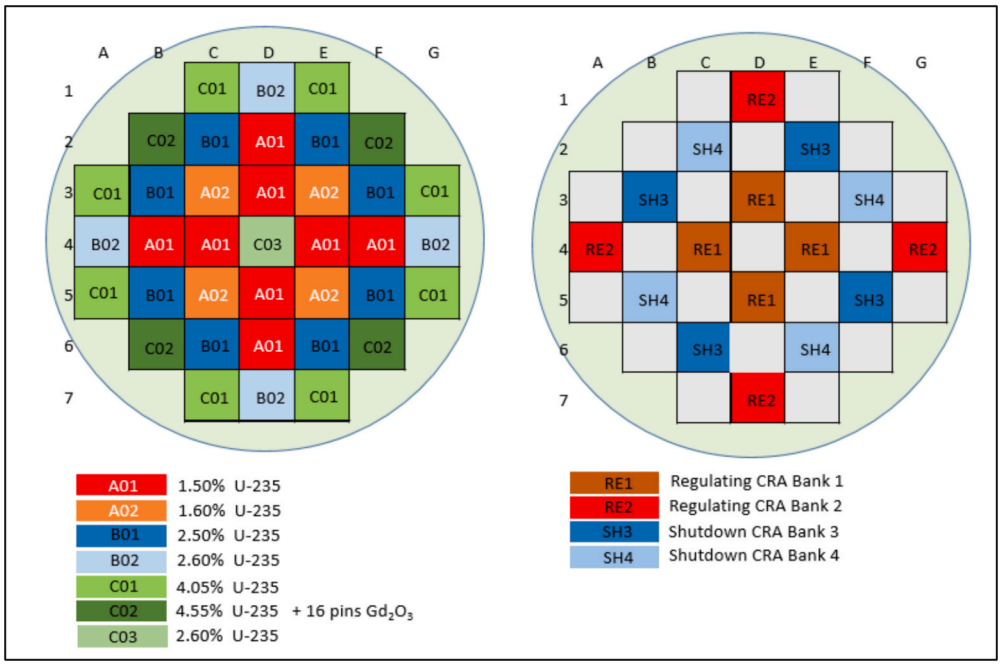

Fig. 1. Initial core loading with UO_2 fuel assemblies (left) and control rod assembly locations (right). Dimensions are given in cm.

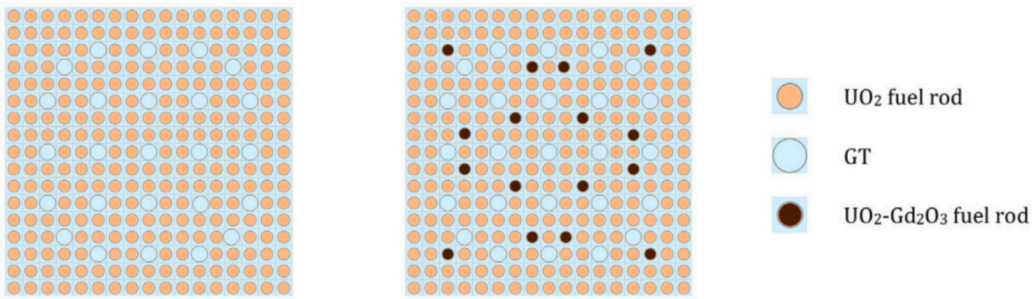

Fig. 2. Radial layouts of fuel assemblies without (left) and with gadolinium rods and guide tubes (right).

supports mixed MPI/OpenMP parallelisation, which was intensively used in this modelling.

In the coupled mode, the SSS estimated the power field, which was transferred to other codes. From coupled codes, SSS received fuel and coolant temperature as well as coolant density fields. These inputs were used for neutron transport modelling in subsequent transient time steps in order to account for the Doppler feedback effect for instance. The field transfer is shown in Fig. 3.

3.2. SUBCHANFLOW

SUBCHANFLOW (SCF) is a four equations (mass, energy, axial and lateral momentum) subchannel thermal–hydraulic code developed and validated at the Karlsruhe Institute of Technology (Imke and Sanchez-Espinoza, 2012). The 3.6.1 version of the code, which was earlier extended with the ICoCo interface, was used in this coupling. SCF is designed to analyse thermal–hydraulic phenomena within the reactor core under steady-state and transient conditions. The program applies empirical correlations related to pressure drops, heat transfer, etc. The reactor core was divided into 10,693 subchannels, regions between the fuel rods where the coolant flows. Each subchannel was treated individually, allowing for detailed simulation of coolant flow and temperature distribution. The subchannel modelling principle in the reactor core is illustrated in Fig. 4. The picture shows one fuel assembly setup with yellow assigned guided tubes.

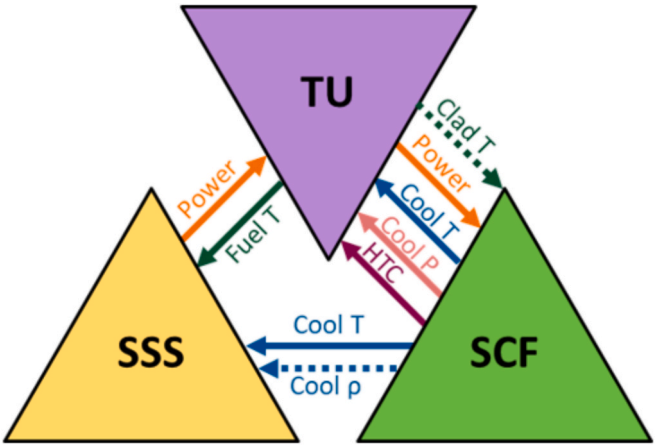

Fig. 3. Filed transfer in the coupled SSS-SCF-TU modelling.

The current SMR core setup contained 9768 fuel rods and 10,693 channels between and around the rods. The SCF was applied in two modelling phases. In the first stationary phase, SCF was run in steady-state mode, and in the second phase of modelling, in transient mode. Throughout the simulation, SCF received cladding temperature and

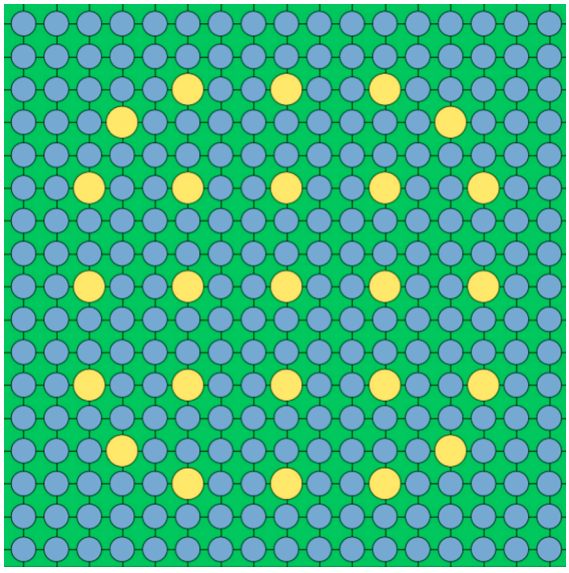

Fig. 4. The subchannel model of the fuel assembly. The guide tubes are shown in yellow.

cladding power from TU, and in return, it transferred coolant temperature and density fields to SSS. Additionally, SCF provided the coolant temperature, pressure, and heat transfer coefficient (HTC) fields back to the TU code, as depicted in Fig. 3.

3.3. TRANSURANUS

TRANSURANUS (TU) is a fuel rod performance code developed at the JRC Karlsruhe (Lassmann, 1992). The version of the TU code applied in this modelling was the v1m3j22 extended with the ICoCo interface. The basic TU kernel code models the dynamic behaviour of individual fuel rods, primarily focusing on thermal and mechanical aspects. The code can analyse fuel, cladding, coolant and structural components. A fuel rod is segmented into axial slices, as shown in Fig. 5. The analysis is done by iteratively solving one-dimensional radial and axial conservation equations, resulting in a 1.5-dimensional approach. Each axial slice is divided into radial rings for enhanced mechanical analysis. This configuration together with inner and outer boundary conditions lead to a system of nonlinear equations. TU calculates the stresses, strains, corresponding deformations and fission gas release among others. The one-dimensional radial mechanical modelling assumes the plane strain approximation and uniform elastic properties within each cylindrical ring. The approach reduces the computation time compared to 3D modelling, allowing the comprehensive simulations of a high number of fuel rods in full core modelling. In this study, each rod was divided into 20 axial slices. Inputs to the single rod modelling included the fuel rod fabrication and material properties for each rod type and dynamic inputs of power and coolant temperature profiles.

For the modelling of UO_2 rods, the standard material properties of UO_2 fuel have been used, whereas for ATF the TU has been extended with corresponding material properties and correlations found in the open literature. Specifically, the elastic modulus for fresh U_3Si_2 fuel is based on the work of Frazer et al. (Frazer, 2021). At the same time, the heat capacity at constant pressure for U_3Si_2 fuel is derived from White (White, 2015) and is a linear function of the absolute temperature. The stationary creep rate of U_3Si_2 fuel is supposed to consist of a thermal creep term, according to Yingling et al. (Yingling, 2021), and an athermal creep term, according to Liu et al. (Liu et al., 2023).

The model for thermal conductivity in U_3Si_2 fuel is dominated by the electronic term. Hence, it increases linearly with the absolute temperature in accordance with the Wiedemann-Franz law. The porosity

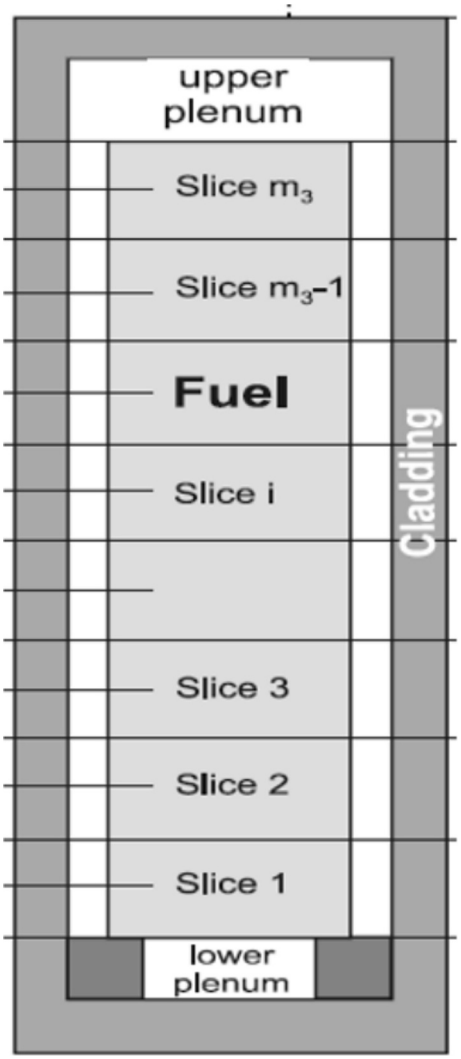

Fig. 5. Axial modelling of a single rod in TRANSURANUS.

correction relies on the Maxwell-Eucken model 1 from Gong et al. (Gong, 2013), as suggested in the recent analysis of measurements by Pavlov et al. (Pavlov, 2021), but assuming a zero thermal conductivity of the pores/bubbles (rather than using 0.02 W/mK as applied by Pavlov et al.). The thermal conductivity degradation with burnup is disregarded for normal LWR conditions, based on the observations of Zhang et al. (Zhang and Andersson, 2017) in the temperature region of interest. Furthermore, the thermal conductivity of molten U_3Si_2 fuel is also disregarded here in view of the limited temperature range of the measurements ($T < 1773$ K) in White et al. (White, 2015). The model for the thermal strain of U_3Si_2 fuel is based on data reported for the coefficients of thermal expansion as a function of the temperature (i.e. average linear thermal expansion coefficient in the anisotropic material) reported by Ulrich et al. (Ulrich, 2020) and Obbard et al. (Obbard, 2018). More precisely, the final linear expression given by Ulrich et al. (Ulrich, 2020) is integrated, starting at room temperature, in order to provide the thermal strain as a function of temperature by means of a second-order polynomial. The cladding properties for FeCrAl in this work have been taken from NINE (Mannan, 2003; Cherubini et al., 2019) in the frame of the ACTOF project of the IAEA. The modelled ATF material properties have been tested in a single rod modelling of a PWR fuel and reported in (Van Uffelen et al., 2023). Table 3 summarises the developments and tests performed on the TRANURANUS code to enable the thermo-mechanical modelling of the ATF discussed in this study.

To run parallel analyses for many fuel rods in full-core modelling, the

Table 3
TU developments for thermo-mechanical modelling of ATF.

TU extension	Reference	Comment
U_3Si_2		
elastic modulus	Frazer et al. (Frazer, 2021)	
heat capacity at constant pressure	White et al. (White, 2015)	linear function of the abs. temp.
thermal creep rate	Yingling et al. (Yingling, 2021)	
athermal creep rate	Liu et al. (Liu et al., 2023)	
thermal conductivity	Wiedemann-Franz law	dominated by the electronic term
porosity correction	Pavlov et al. (Pavlov, 2021), Gong et al. (Gong, 2013)	Maxwell-Eucken model 1,
thermal strain	Ulrich et al. (Ulrich, 2020), Obbard et al.(Obbard, 2018).	
FeCrAl		
all properties	Mannan, S., et al. (Mannan, 2003); Cherubini, M. (Cherubini et al., 2019)	
modellig in TU	Van Uffelen, P., et al. (Van Uffelen et al., 2023)	single rod modelling plus uncertainties

basic TU kernel code has been incorporated into a wrapper program that runs an instance of the TU kernel for each fuel rod. Each TU instance processes input parameters at the start of a time step and produces output results of the iterated time step. The rod/slice position in the core mesh is important because, based on that, the TU kernel receives the power data from SSS and coolant conditions from SCF and returns the fuel temperature to SSS and cladding temperature and heat flux (power) to SCF. The transferred scalar fields are shown in Fig. 3. The configuration allows the retention of detailed mechanical results at the slice and time step level for all individual fuel rods.

3.4. Interface for Code Coupling

The Interface for Code Coupling (ICoCo) was developed in the EU's Research and Innovation Framework Program 7 (FP7), project NURESAFE (Chanaron, 2017). It is an abstract interface of the Nuclear Reactor Simulation (NURESIM) platform (Chauliac, 2011), which is based on the SALOME platform (Salome Platform, 2018). SALOME is an open-source platform that supports the coupling of various solvers. The MED data model is used to exchange numerical fields and meshes.

The ICoCo has an object-oriented design with a MED mesh-based feedback exchange. The primary object in ICoCo is the "Problem". A Problem is a solver; in this study one of the codes SSS, SCF, or TU. The solvers have to be modularised and extended with an interface structure (Fig. 6). ICoCo specifies which methods a Problem has to provide and

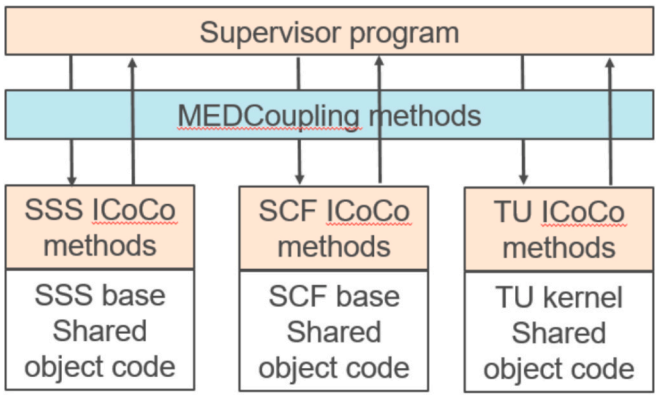

Fig. 6. ICoCo based coupling scheme SSS-SCF-TU.

what those methods are supposed to do in the coupling. The solver's ICoCo methods have to provide a time-dependent solution as a function of input data. The coupling is implemented in a supervisor program that is independent from the solvers. The supervisor calls the provided methods sequentially, and the interpolations and data manipulations are performed after each time step. The monolithic codes SSS, SCF, and TU had to be modularised to be able to continue the modelling, following the data exchanges, in the next time-step calculation. The ICoCo adaptations of the SSS, SCF and TU codes are described in detail in the deliverables of the McSAFE project (Sanchez-Espinoza, 2021).

The ICoCo methods, added to the solvers, are doing the initialisation, termination, time iterations and field manipulations. Table 4 summarises the most important methods added to each code to realise the coupling.

3.5. MED data model

The ".med file" format and the library named MEDCoupling were used in this coupling. We used the 7.8.0 version of the MEDCoupling that provides structures to manipulate and hold the scalar fields in memory. A Python pre-processor has been developed to generate the synchronized basic MED meshes for each code. The fuel rods and the coolant channels have been indexed. Additionally, a table mapping fuel and coolant channels was generated. All the channels and fuel rods were divided into 10 cm axial slices, and their position layouts were prepared. It is worth mentioning that inside a time step, the SCF calculates the fields in horizontal layers, whereas TU calculates each rod separately in the axial direction. Therefore, mapping layers to fuel rod slices in TU plays an important role.

3.6. Coupling methodology

At the beginning of the study, the Serpent2 input files were prepared with NuScale core's geometry, material descriptions, and rod movement scenarios. SUBCHANFLOW input included synchronised cooling channel descriptions, and the TRANSURANUS code was modified to include new material properties and correlations for ATF. The fuel pins were divided axially into 10 cm slices, which corresponded to the data transfer meshes in the coupling. To model the radial temperature distribution, stresses and strains in TRANSURANUS, we set up 25 mesh points for fuel and 12 mesh points for cladding.

A separate main program was developed that initialises the supervisor, the solvers (SSS, SCF and TU), and starts the coupling. Inside the supervisor program, the solvers are sequentially called in the order defined in the input file. The same input file describes the fields

Table 4
The most important ICoCo methods added to the coupled codes.

Method	Description
Problem	Constructor and destructor of the engine
setDataFile	Give the name of a data file
setMPIComm	Give an MPI communicator to the code
initialize	Initialise the code using the arguments of setDataFiles
terminate	Terminate the computation, free the memory and save the results
presentTime	Return the current modelling time t
computeTimeStep	Return the preferred time step or tells that the code wants to stop
initTimeStep	Give the next time step to the code
solveTimeStep	Perform computation on the current interval, with the current time step
validateTimeStep	Validate the computation performed by solveTimeStep
abortTimeStep	Abort the computation of current time step
getInputFieldNames	Return a list (string) of field names identifying input fields of a code
getOutputFiledNames	Return a list (string) of output field names
setInputField	Provide an input field
setOutputFiled	Return an output field

transferred between the codes (Fig. 3). The order of the solver is SSS-TU-SCF. Putting the TU directly behind SSS, we could model the power transfer delay resulting from sudden power changes during the transient.

The modelling process had three phases (Fig. 7):

1. **Critical Boron Concentration Calculation:** In the initial coupled phase, SSS, due to several iterations, determined the critical boron concentration in a stationary steady state of the core.
2. **Initial Source Generation:** In the second phase, the SSS program was used in single-run mode in order to prepare the initial source file for the transient mode.
3. **Transient Simulation:** In the final phase, SSS simulated a 4-second long REA event using 2 ms time steps. The power field was transferred to TU for each time step, which executed the time step. After that, TU forwarded to the SCF code the cladding temperature and heat flow from the cladding, while SSS received the rod temperature as a feedback field from TU along with the coolant temperature and density from SCF to compute the fission power field for the subsequent time step.

Before starting the transient mode, a 48 h long steady-state iteration between SCF and TU was performed for conditioning of the rods, and fields generated in this step were uploaded to the transient part of the modelling.

The application of the high-resolution, detailed modelling was made possible by the availability of High Performance Computers (HPC). Despite significant computational capacities, we needed substantial runtime for the simulation. However, compared with the less time-consuming low-order methods, the advantage of the high-order pin-by-pin approach is that it applies fewer approximations of the reactor core behaviour. One can check the detailed behaviour of each single fuel rod inside the core, thereby reaping the benefits from the state-of-the-art fuel performance codes to describe the detailed fuel rod behaviour with conventional fuel or ATF.

To prepare this study we developed and tested code modifications in ICoCo methods and in the supervisor program to be able to perform transient modelling of sub-sequential time steps as follows:

- SSS first solves the time step and calculates the fission power.
- The supervisor transfers the power fields to TU.
- TU performs the time step for each rod.
- The supervisor transfers the cladding surface temperature and cladding-to-coolant power fields to SCF.
- SCF performs the time step for each channel.
- The supervisor transfers the coolant temperature, pressure and heat transfer coefficient fields to TU and coolant temperature/density, fuel temperature to SSS (Fig. 3).
- SSS simulates the CR movement and starts the next time step

During the transient, we modelled 2000 time steps of 2 ms for a total of 4 s modelling time. Calculations were conducted on seven nodes with 42 3.00 GHz CPUs on each node. The first stationary step, to calculate the critical boron concentration, took around two hours with 1000 active generations of neutrons and 500,000 neutrons per generation. The initial source generation (second step) needed around 15 min with the same population setup. The most time-consuming part was the transient part, which needed around 21 h of running time, with 10^6 neutrons in each 2 ms long time step. Around 50 % of the computing time was needed for SSS and the other 50 % for TU plus SCF calculations. During the simulation, approximately 40 GB of modelling data was generated for a single REA case with one fuel type. A total of 100 GB of RAM was allocated, primarily for the Monte Carlo neutronics calculations and for the parallel execution of 9768 TU instances, one for each fuel rod.

The original TU is a code for single rod modelling. To enable the parallel calculations of many fuel rods in full-core applications, a wrapper was developed to generate an indexed array of TU kernel instances. The first version of this wrapper and the additional modularisation of the code were added to the TU version of 2015. In this study, we added the wrapper to the newest version of the code and made the necessary modifications inside the code. In the full-core and multi-rod modelling, the wrapper generates an indexed array of TU kernel instances and distributes them between the available HPC nodes. Each of the instances can model a single fuel rod in the full core. To have the global variables available for the subsequent time steps and final data exchange, additional subroutines were added to the TU's ICoCo interface, defining all the global variables of the parallel running TU instances. The global variables in the original TU source code were replaced by pointers that point to the variables of the indexed TU instance. In this way, the individual rod simulation worked well in full core parallel processing. The results were collected in MED fields.

4. Modelling scenarios

Two REA transient scenarios for two core loading with conventional fuel (UO_2) and ATF (U_3Si_2) have been modelled. The first scenario (REA1) assumes a control rod ejection within 0.1 s at 75 % nominal power. The second scenario (REA2) assumes that the rod ejection occurs at HZP conditions (Valtavirta, et al., 2021). Both scenarios were applied to fresh-loaded fuel following 48 h of steady-state modelling, with a

Table 5
The enrichment levels of the two different fuel types. The UO_2 column shows the enrichment of the conventional fuel rods. It is same to data shown in Fig. 1. The U_3Si_2 column presents the modified enrichment for each fuel rod type used in the ATF core load.

Rod type	UO_2 (wt% ^{235}U)	U_3Si_2 (FeCrAl clad)
A01	1.50	1.47
A02	1.60	1.57
B01	2.50	2.52
B02	2.60	2.58
C01	4.05	4.30
C02	4.55	4.55
C03	2.60	2.58

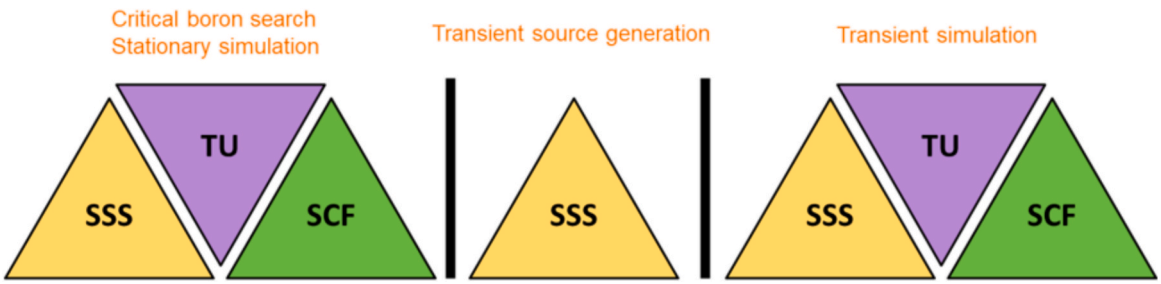

Fig. 7. The three steps for SSS-SCF-TU simulations in NuScale rod ejection event.

critical boron concentration in the coolant. As the Table 5 shows, the enrichments of ATF rods were slightly different. These differences were based on the preliminary calculations aimed at reaching a similar maximal power level in the transient for the different fuel rods when taking into account differences in fuel density. These initial conditions were not perfectly reached, as can be seen in the result section. A sensitivity analysis would be needed to improve the modelling inputs in this sense, but this is computationally very expensive and beyond the scope of this paper.

The first scenario (REA1) started from the steady-state at the core power level at 75 % (120 MWth), with critical boron concentration. The CRAs RE1, SH3, and SH4 were fully withdrawn, and the bank RE2 was withdrawn at 56 %, as shown in Fig. 8. The transient started with the ejection of a single control rod (CR) in the RE2 bank located in A4. The ejection took 0.1 s, and the SCRAM started after 2 s. This scenario assured a sudden increase in the fission power to around 100 % of the core nominal power of 160 MWth.

The second HZP scenario (REA2) started at the core power level at 0.1 % of nominal power, in a steady state, and with critical boron concentration. All the CRAs were 100 % withdrawn except for the RE2, which was withdrawn to the 25 % level (Fig. 9**)**. The CR of type RE2 ejected was located in A4. SCRAM followed in the same regime as in REA1. The scenario generated a sudden increase in the fission power above several hundred per cent of the nominal power.

In both scenarios and for both fuel types, we modelled a steady-state prior to the transient. During this step, SSS calculated the critical boron concentration in several iterations. Based on the critical concentration, a single SSS run generated the initial live neutron and delayed neutron precursor sources needed for the transient. The transient modelling started with the uploading of steady-state fields, and used the initial source for power field generation. The field exchange was performed in every 2 ms during the transient.

In the first steady-state modelling step, all thermal processes were in balance, which means that the power deposited in fuel pellets was equal to the power transferred from the cladding surface to the coolant. On the other hand, during the transient, the local heat balance is not conserved; the power transferred from the cladding to the coolant may differ from that deposited in the pellet due to the time constant for the heat transfer in the fuel (seconds) that is much larger than the REA pulse width. Therefore, the heat flux from the cladding to the coolant must be calculated in the TU ICoCo modules. The field was calculated for each axial slice of each rod based on the following formula:

$$P = 2 \bullet \pi \bullet R_{clad} \bullet dz \bullet HTC \bullet (T_{clad} - T_{cool})$$

where R_{clad} is the cladding outer surface radius, dz is the axial slice length, HTC is the heat transfer coefficient from SCF, T_{clad} is the cladding outer surface temperature from TU, and T_{cool} is the coolant temperature from SCF.

5. Results and discussions

The ejected control rod worth (CRW) of UO_2 and ATF cores for both considered scenarios were estimated in a stand-alone Serpent2 isothermal calculations with core-averaged fuel and coolant temperatures and shown in Table 6.

Fig. 10 **(left)** shows the total fission power for both types of cores (UO_2 and ATF) during the first REA1. The power evolution during REA1 for both considered cores is similar: sharp power increase due to rod ejection between 0 and 0.1 s, than slight decrease of power between 0.1 s and 2 s and finally sharp decrease starting from 2 s due to SCRAM insertion.

As can be seen, the ATF's core power peak is slightly below that of the UO_2 core, which corresponds to slightly lower reactivity introduced in rod ejection (see Table 6). The statistical fluctuations shown in this figure are the peculiarities of the Monte Carlo neutron transport methods. In both cores, a weak power peak can be observed at the very beginning of the transient that drops after 0.01 s. The peak is higher than the fluctuations. The reason is not yet clear and could be due to a data transfer problem between the steady state and transient modes. To analyse this peak, further tests are planned to increase the time and space resolution in this part of the modelling.

Fig. 10 on the right shows the time evolution of the fuel maximal temperatures in the core. It can be seen that the curves for UO_2 and ATF follow the same pattern, reaching the maximum at 2.2 s, although in the ATF core the maximal temperature is around 320 K lower. Because the maximal coolant temperature in both cores was almost the same and almost constant during the modelling, around 594 K, the ATF's better thermal conductivity can largely explain this temperature difference, in addition to the lower power peak in the ATF core. The effect of the thermal conductivity of the ATF selected here has previously been analysed during normal operation conditions in a commercial NPPs (Van Uffelen et al., 2023).

To present the possibilities of the high-resolution modelling, Fig. 11 shows the colour-coded spatial distribution of temperature at 2.2 s. It can be seen that overall in the ATF core the local maximum temperature was lower.

Using the TU post-processing tools, we performed the intra-rod analysis near the ejected CR at the position shown by the red arrow in Fig. 11. A C01-type, higher-enriched fuel rod was selected for that purpose. In the conventional UO_2 core, the U-235 enrichment of the C01 was 4.05 %, and in the ATF core, it was 4.30 % (see Table 5).

Fig. 12**,** on the top left, shows the linear heat rate profile generated

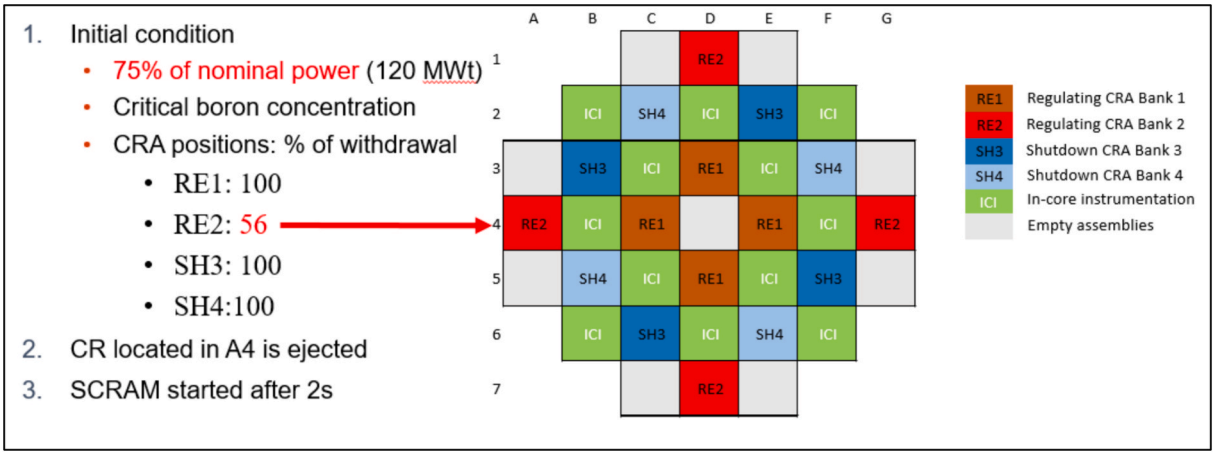

Fig. 8. The first REA1 scenario.

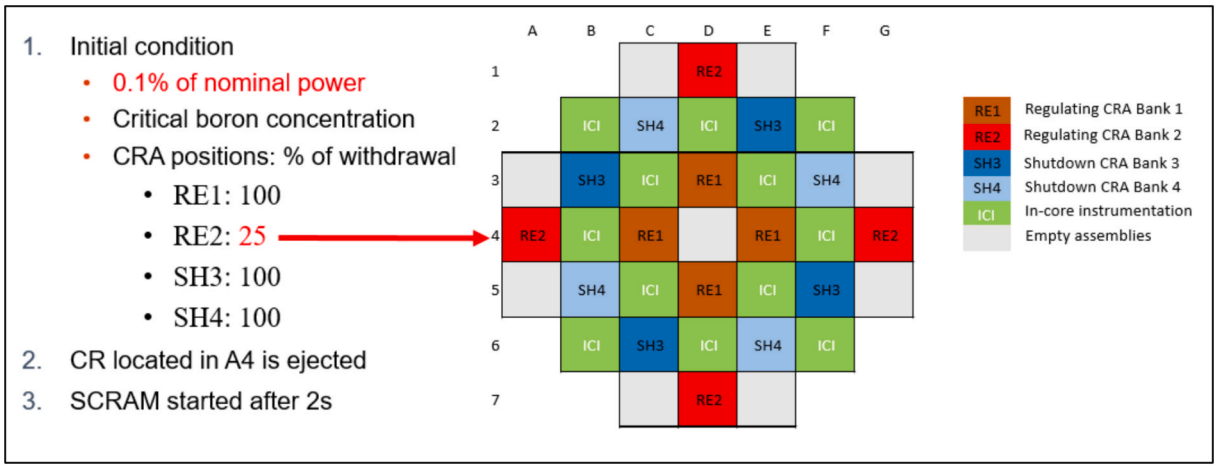

Fig. 9. The second REA2 scenario.

Table 6
Static reactivity coefficient.

Scenario	Core	CRW, pcm
REA1	UO_2	171.82 ± 2.46
	ATF	166.00 ± 2.53
REA2	UO_2	726.55 ± 2.46
	ATF	708.94 ± 2.55

based on the SSS power distribution and transferred to the rod's mid-height position to TU at axial slice 10. The linear heat rate provided by SSS typically shows the fluctuations of Monte Carlo calculations that can be reduced by increasing the number of simulated neutrons (at the expense of more computation time). Despite the higher enrichment, the power peak was slightly lower in the case of ATF. The top right plot shows the maximal fuel temperature and the bottom left plot shows the evolution of the gap size over time at the same location. The smaller gap size leads to a higher gap heat transfer and as a result to a lower fuel temperature and higher coolant temperature shown on the bottom right plot in Fig. 12. The time constant of the fuel temperature was measured with central thermocouples during a SCRAM in the experimental Halden Boiling Water Reactor to be around 2 s. This explains why the power fluctuations provided by SSS are filtered out in the temperature calculations of TRANSURANUS.

The fuel temperatures of UO_2 and ATF follow a similar pattern, with around 220 K constant higher temperature in the case of UO_2. This fact proves again the better thermal conductivity of the ATF. The gap size is lower in the ATF thanks to the higher strength of FeCrAl. In the shutdown phase, which starts after 2 s, the gap in ATF grows faster than the gap in UO_2 fuel thanks to the modified differential thermal expansion and elastic properties of the materials.

The second REA2 scenario modelled an accident with a higher but shorter power peak. In this scenario, the core power suddenly increased from 0.01 % to over 600 % in the UO_2 fuel core and over 300 % in the ATF core, as shown in Fig. 13. In this scenario, the full-core power difference between UO_2 and ATF is even higher than in the REA1, which corresponds to slightly lower reactivity introduced in rod ejection (see Table 6).

Further research would be needed to find a setup that provides a similar power peak for both types of fuel, which is beyond the scope of the present paper. Fig. 14 shows the evolution of the fuel maximal temperature for UO_2 and ATF in two scenarios. It can be seen that the maximum fuel temperature in both scenarios is lower for ATF, largely due to the better thermal conductivity of ATF. The temperature difference in two scenarios is more significant in the case of conventional UO_2 fuel than in the case of ATF cores, due to the less intensive power peak

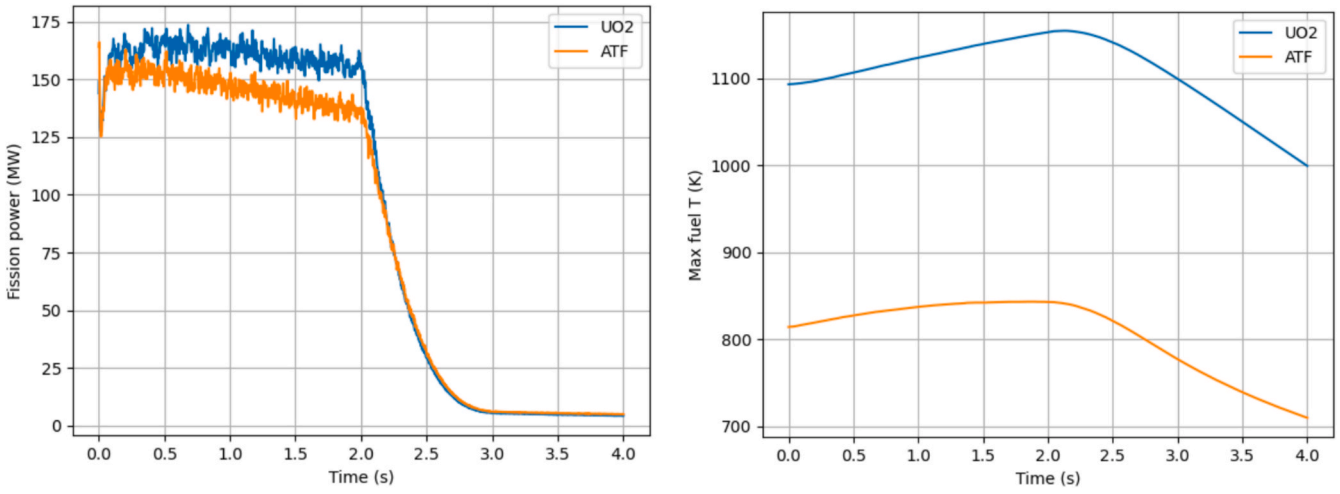

Fig. 10. Evolution of the total fission power during the REA1 transient, with reactor SCRAM initiated after 2 s (left), and the corresponding maximum fuel centreline temperature in the core (right). The data were derived from scalar field values generated by Serpent2 and TRANSURANUS, taking into account the feedback effects of the coupled system at each time step.

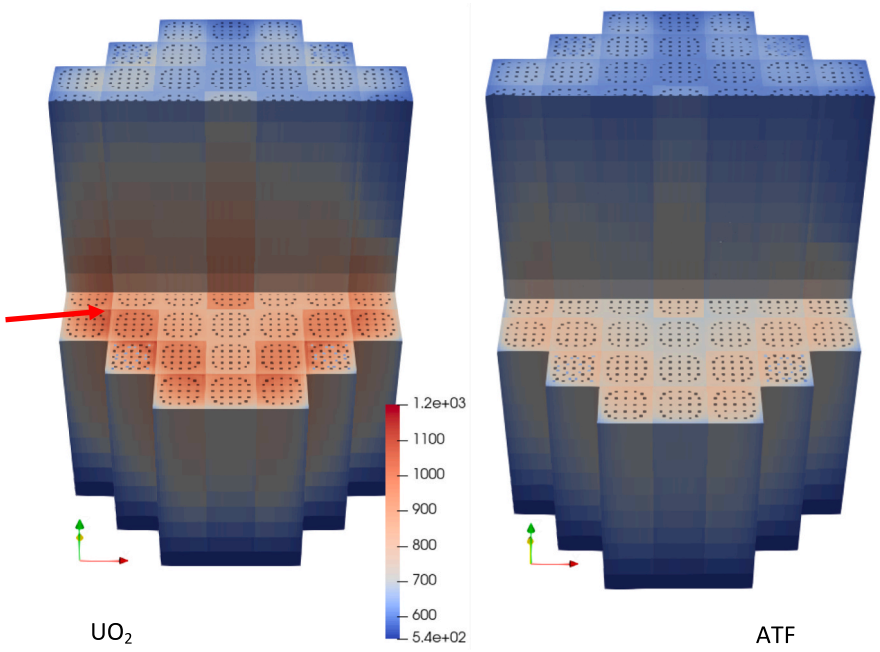

Fig. 11. Fuel rod maximum centerline temperature 2.2 s after the onset of the REA in the non-ATF (left) and ATF (right) core.

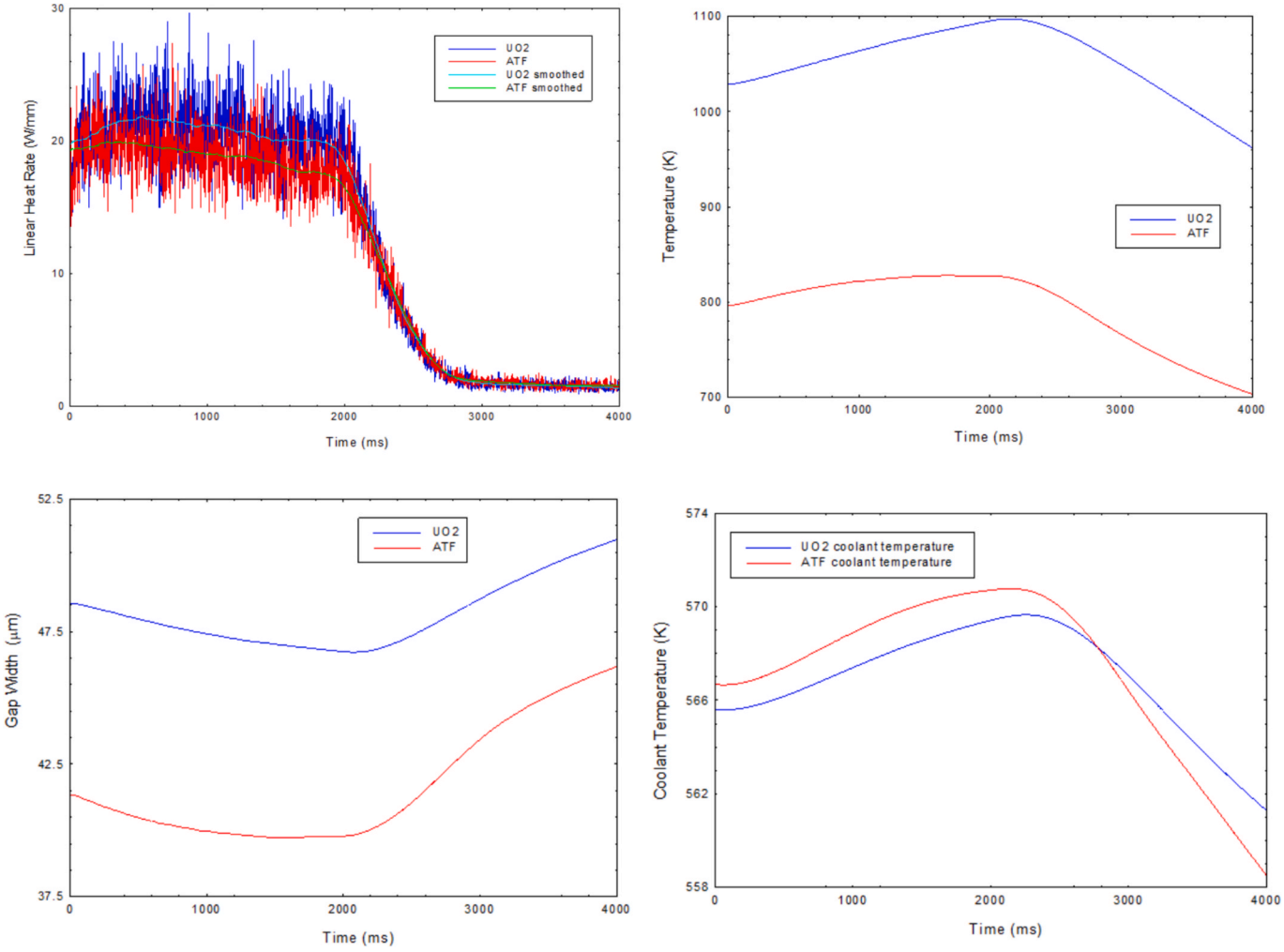

Fig. 12. Time evolution of the linear heat rate (top left), maximum fuel temperature (top right), fuel–cladding gap width (bottom left), and coolant temperature (bottom right) at the axial mid height of a selected fuel rod. The data were extracted directly from TRANSURANUS output files.

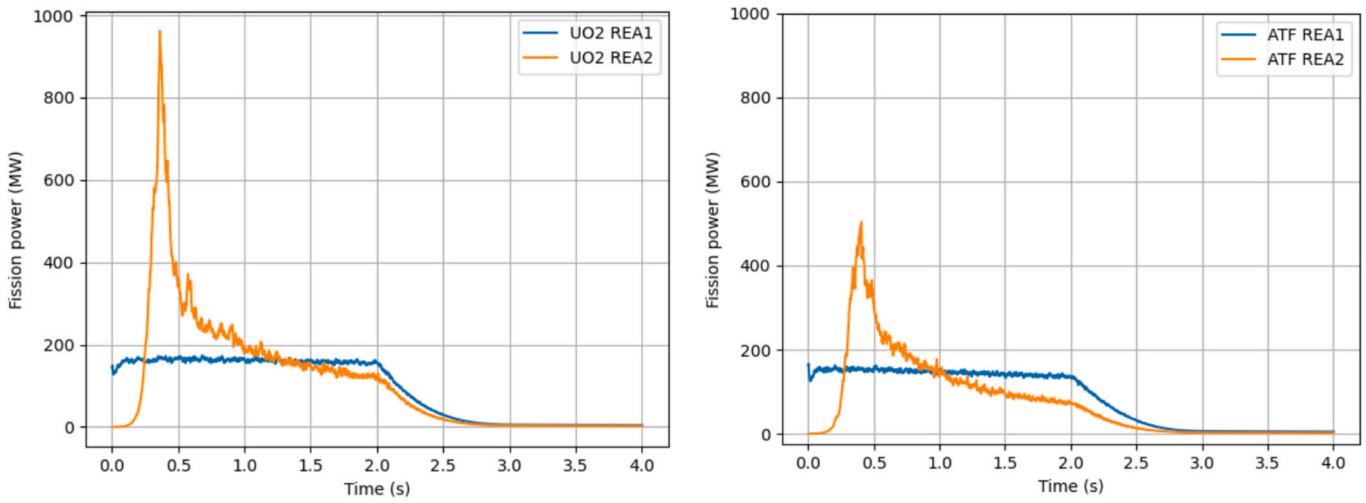

Fig. 13. Fission power of two scenarios, UO_2 fuel (left) and ATF (right). The data were derived from scalar field values generated by Serpent2, taking into account the feedback effects of the coupled system at each time step.

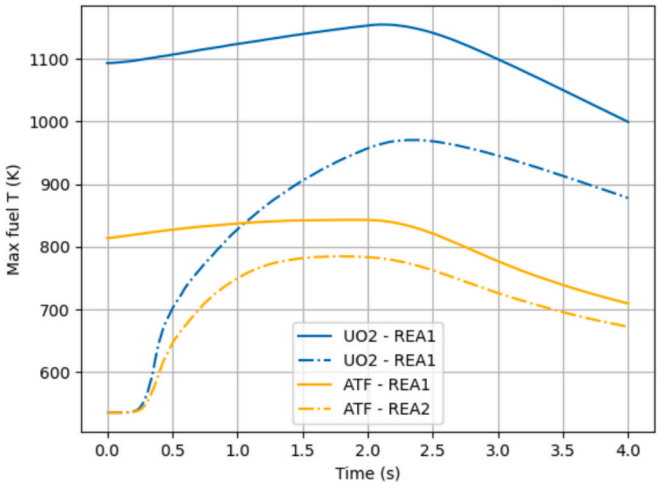

Fig. 14. Fuel maximal temperature for UO_2 fuel and ATF in two REA scenarios. The data were derived from scalar field values generated by TRANSURANUS, taking into account the feedback effects of the coupled system at each time step.

for the ATF in REA2 scenario.

The distribution of the temperature differences between conventional fuel and ATF has also been investigated, as shown in Fig. 15. In the REA1 case (left), the maximum local differences can be observed in all outer assemblies of the core. On the other hand, in the REA2 case, the maximal local difference between UO_2 and ATF appeared in the assemblies around the REA event. This can be explained by the fact that the power peak in the REA2 was shorter and influenced only the vicinity of the ejected CR.

Using the TU data, we compared the mid-height intra-rod modelling results near and far from the ejected rod for the same type of fuel rod. Fig. 16 left shows the maximal fuel temperature evolution in a slice that represents a 10 cm long piece of the fuel rod near the rod ejection event. The red curves show the ATF, and the blue curves show the UO_2 maximum axial temperatures in two scenarios. These local temperature curves are very similar to those showing the full core maximal temperatures in Fig. 14. It can be seen that at this location, the UO_2 rod temperatures were significantly higher than those of the ATF, albeit far below the melting temperature. Fig. 16 right shows the local mid-height temperature far from the REA event. All the temperatures are lower than near the Ejected CR. The difference between ATF and UO_2 is lower in the REA2 event, in which the starting power was much lower but with a shorter and higher power peak. This investigation shows that the high-resolution coupled codes used here are able to predict local safety parameters in a direct manner compared to nodal-level simulations. This example indicates that the local evolution of key parameters can differ depending of their position within a fuel assembly and core, highlighting the importance of detailed pin-by-pin full core simulations for safety

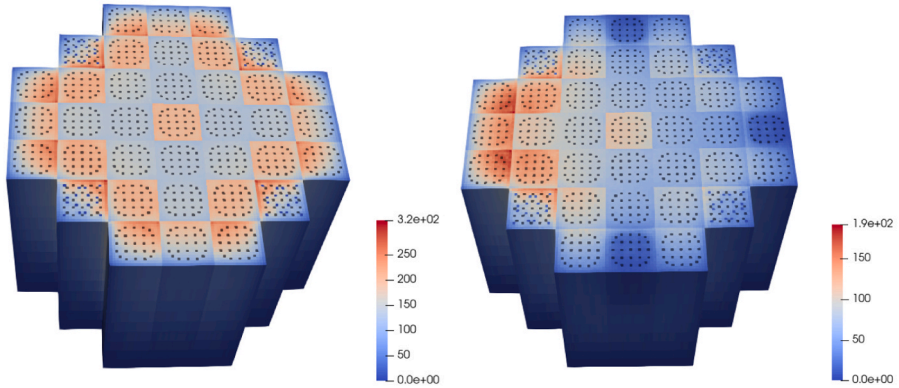

Fig. 15. The local maximum core temperature difference between UO_2 fuel and ATF at the mid-height of the core, on the left – REA1 and on the right REA2 case.

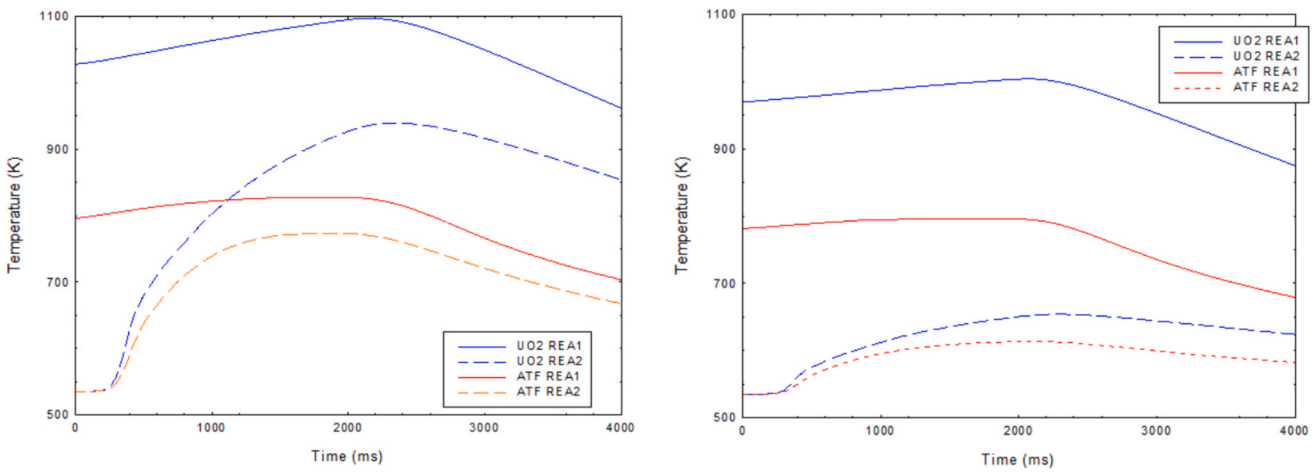

Fig. 16. The local inner fuel maximal temperature near REA (left) far from the Ejected CR (right). The data were extracted directly from TRANSURANUS output files.

analysis.

Fig. 17, on the left, shows the changes of the local gap width and HTC during the transients, which is only possible thanks to the inclusion of TRANSURANUS in the coupled code system. The gap widths are calculated only in TU and are not transferred to other codes. It can be seen that the gap is bigger in the UO_2 rod. In the REA2, the gap reduction is more pronounced, and the smallest gap is in the ATF during the REA2 scenario. Fig. 17, on the right, shows the different gap conductance as a function of time, confirming that the local conductance is higher if the gap is smaller.

Fig. 18 shows changes in the gap width in different REA for different fuel types and in different rod positions. The fuel rod is type C01, and it is located near the Ejected CR. The position L2 is at the bottom, the *L*10 is at the middle, and the L19 is at the top of the fuel rod. The initial uniform gap width was 80 μm.

In each scenario, as it was mentioned earlier, we simulated a 48-hour long steady-state of the fresh fuel rods before the transient. The plots on the top show the gap width during the REA1 scenario, on the left for UO_2 fuel, on the right for ATF, and on the bottom the same results during the REA2 scenario. The ATF fuel had a smaller gap at the beginning of the transient. Some significant but not dramatic gap changes can be observed at the mid-height of the fuel rods (red curves). In the REA1 scenario, in the shutdown phase, after 2000 ms, the ATF showed intensive gap growth. In the REA2 scenario, in the power peak phase, until 1000 ms, the ATF showed more intensive gap reduction. This analysis illustrates the benefit of coupled modelling that includes TRANSURANUS with detailed rod behaviour modelling. Fig. 19 shows that the ATF types of the fuel rods have higher expansion near the Ejected CRs.

The analysis above also points out the need to consider such coupled high-fidelity calculations when analysing design basis accidents in water cooled SMRs when experimental data are scarce. In particular, in absence of data about the reactivity insertion in the reactor loaded with ATF, and applying the same power pulse as that in the core loaded with conventional fuel during a REA may be misleading: Liu et al (Liu et al., 2023) assumed the same power pulse for both fuel types and predicted melting to occur in the U_3Si_2 fuel pellet, although the results presented here indicate a lower peak height so that melting in U_3Si_2 fuel in pellet during RIA may not happen due to the reduced power peak in ATF.

6. Summary and conclusions

This work was carried out as part of the McSAFER project, which builds on the code coupling system developed in the earlier McSAFE project. In that project, the ICoCo-based Serpent2-SUBCHANFLOW-TRANSURANUS coupling approach was created to perform high-fidelity, pin-by-pin static and depletion calculations for LWR cores loaded with conventional fuel. In the subsequent McSAFER project, several key extensions were made to this approach to enable the modelling of SMRs under transient conditions, using both conventional UO_2 fuel and ATF. These extensions include the introduction of a new SMR core geometry, along with material properties and correlations for

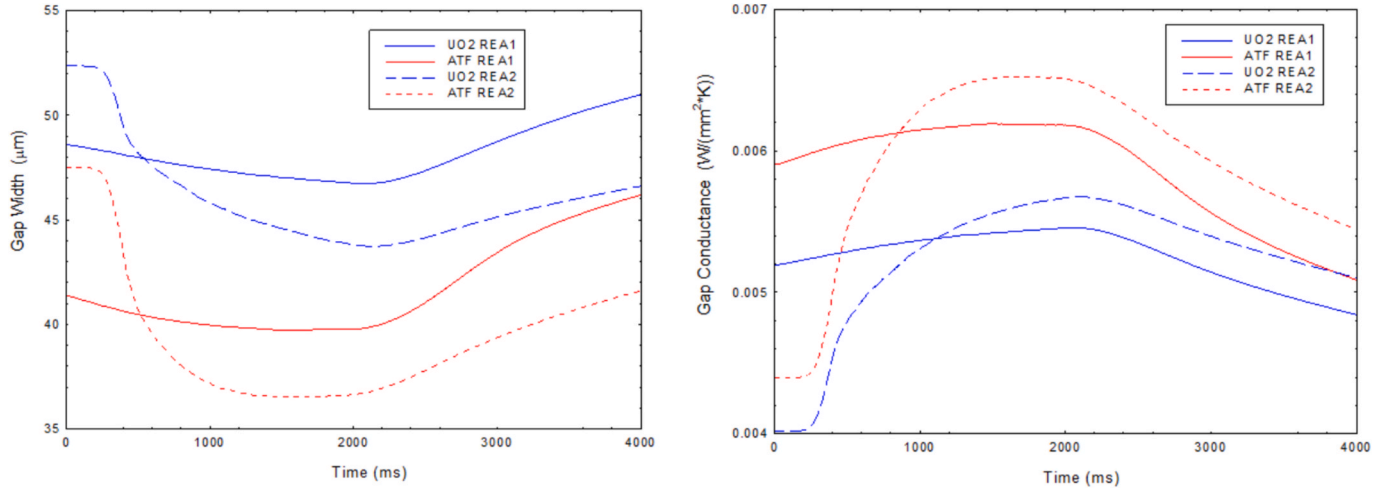

Fig. 17. Local gap width and gap conductance in both scenarios and for both fuel types. The data were extracted directly from TRANSURANUS output files.

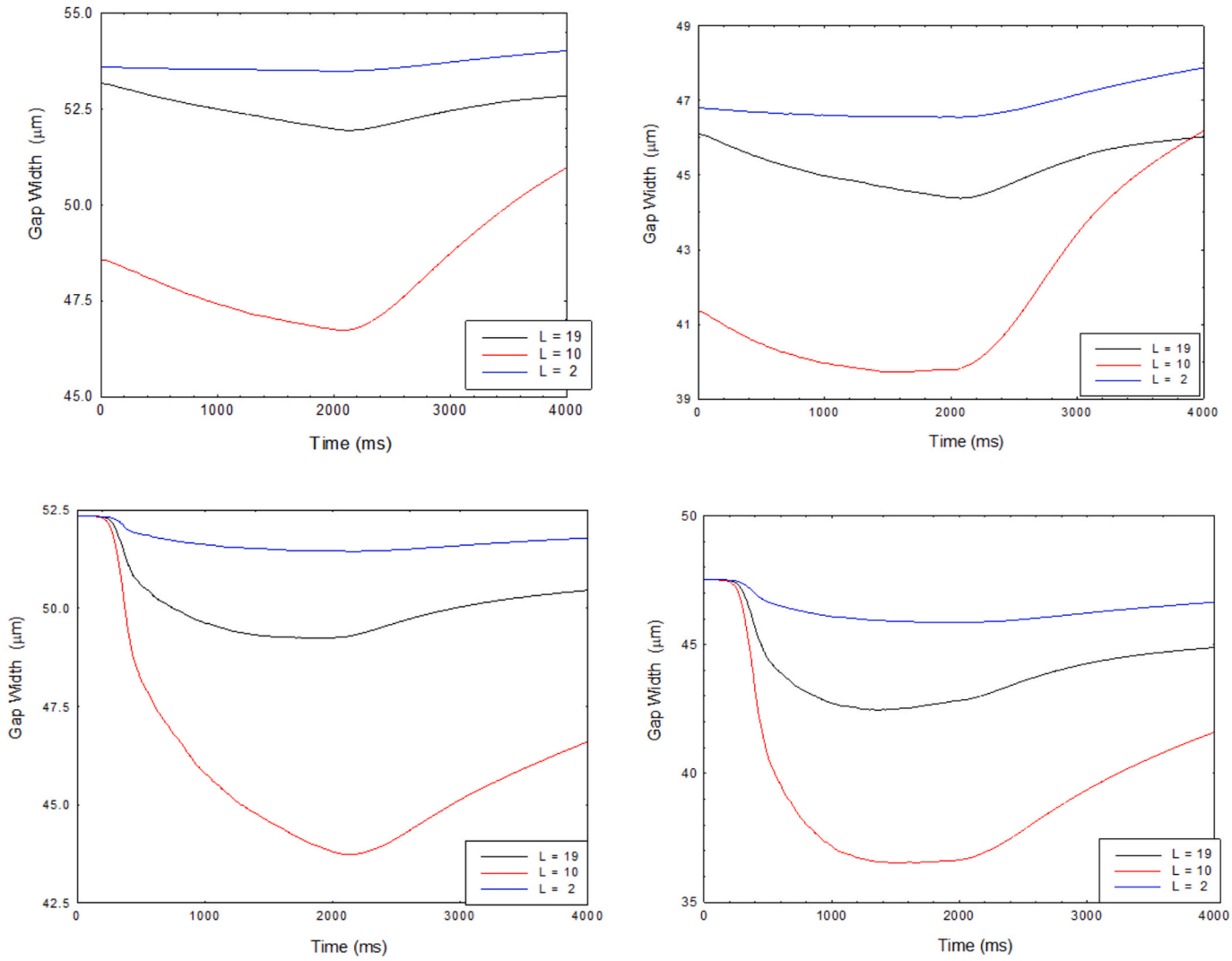

Fig. 18. Gap width as a function of time in two different REA events and for two different fuel types. Top left: REA1 UO_2, top right REA1 ATF, bottom left REA2 UO_2, bottom right REA2 ATF. The data were extracted directly from TRANSURANUS output files.

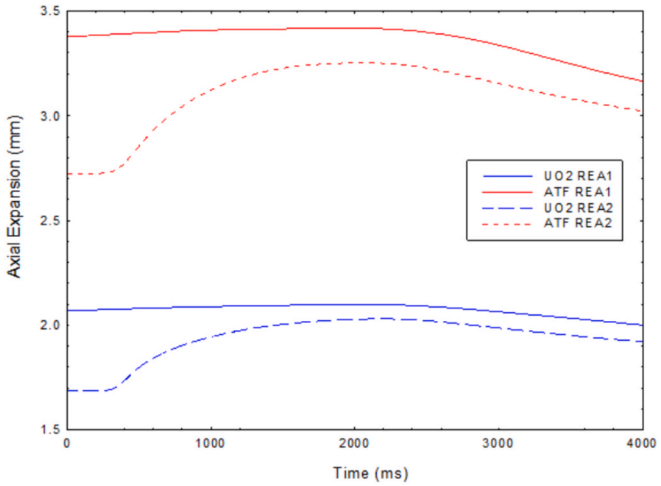

Fig. 19. Axial expansion of different types of fuel rods in REA1 and REA2 scenarios. The data were extracted directly from TRANSURANUS output files.

uranium disilicide (U_3Si_2) fuel with FeCrAl cladding (ATF). Additionally the ICoCo-based coupling was modified to facilitate the analysis of transient scenarios.

Based on this, two rod ejection scenarios were investigated with the extended coupled codes: the scenario REA1 started at 75 % nominal power while the REA2 scenario started at the HZP conditions (0.1 % power). The performed simulations showed that the REA1-scenario leads to a moderate power increase up to 100 % of the nominal power. In the REA2 scenario, the power increase was 600 % for the UO_2-Zr-4 core loading and 600 % for the ATF core loading. Both global and local parameters could be selected for discussions. In two different REA scenarios, no drastic fuel deformations either in global or local mechanical analysis were identified. It was also shown that the energy accumulation in the rod must be modelled in detail along with all its consequences by means of a fuel performance code like the TRANSURANUS code, because in REA transient scenarios, the power transfer from a fuel rod to the coolant occurs much slower than the power generation in the rod. It is worth to point out that one can also reap the benefits from the ATF properties included in such codes. The results showed the impact for the core behaviour loaded with ATF under REA-conditions, which has higher conductivity compared to UO_2, expressed in the reduced power peak compared to the one of a core with conventional fuel. The main challenge remains the calculation cost. The modelling was performed on JRC's HPC Petten, and one calculation took

around one day of computation time.

7. Perspectives

The investigation demonstrated the potentials of the novel Multi-physics coupled code system to evaluate the safety features of SMR-cores predicting local safety parameters. The different input and scenario combinations showed the flexibility and robustness of the coupled system. Nevertheless, additional research is needed to foster the use of such tools by end users and in the licensing process: extend the validation of the coupled tools by identifying appropriate tests, optimize the coupling approach regarding the frequency of data exchange between the involved solvers during the transient simulation, study the impact of the time bins of the Monte Carlo code on the prediction of core parameters, reduce the statistical uncertainty of the coupled solutions, and explore the use of GPUs to speed up the Monte Carlo simulations.

The standardized data exchange and coupling framework enables the implementation of alternative simulation strategies, such as replacing the Monte Carlo solver with a deterministic code to reduce computational overhead, provided the replacement supports an ICoCo-compliant interface. The modular nature of the system also allows its application to other reactor types and designs, such as water cooled and advanced technology SMRs and liquid metal fast rectors, through straightforward input file modifications.

In parallel, future efforts will focus on extending TRANSURANUS capabilities by incorporating additional material properties and models for ATF, thereby expanding its applicability in coupled simulations also to other reactors such as the SMART design. Finally, further investigation is needed to understand better and mitigate artefacts associated with the transfer of field data between steady-state and transient simulations.

Contributions

In this study, we intensively used the software modules developed by colleagues at the Karlsruhe Institute of Technology, Helmholtz-Zentrum Rossendorf-Dresden and VTT Technical Research Centre, Finland. Colleagues at VTT and Lappeenranta University prepared the input files for Serpent2 and SUBCHANFLOW codes. Colleagues at JRC prepared the input files for TRANSURANUS and modified the ICoCo interfaces to model transient scenarios. The modelling was performed on the JRC's High Performance Computer in Petten.

CRediT authorship contribution statement

Zsolt Soti: Writing – original draft, Visualization, Software, Investigation, Conceptualization. **Paul Van Uffelen:** Writing – review & editing, Supervision, Software. **Arndt Schubert:** Writing – review & editing, Software, Resources, Methodology, Data curation. **Ville Valtavirta:** Writing – review & editing, Supervision, Software, Methodology, Data curation. **Riku Tuominen:** Writing – review & editing, Supervision, Software, Methodology. **Heikki Suikkanen:** Writing – review & editing, Supervision, Software, Methodology. **Ville Rintala:** Writing – review & editing, Supervision, Software, Methodology. **Andre Gommlich:** Software, Methodology. **Emil Fridman:** Writing – review & editing, Conceptualization. **Yurii Bilodid:** Writing – review & editing, Visualization, Conceptualization. **Luigi Mercatali:** Writing – review & editing, Visualization, Software, Methodology, Conceptualization. **Victor Hugo Sanchez-Espinoza:** Writing – review & editing, Supervision, Methodology, Conceptualization.

Declaration of competing interest

The authors declare that they have no known competing financial interests or personal relationships that could have appeared to influence the work reported in this paper.

Acknowledgements

This study was performed in the frame of the H2020 project entitled "High performance advanced methods and experimental investigations for the safety evaluation of generic Small Modular Reactors" (McSAFER) the project leader was the Karlsruhe Institute of Technology. The project received funding from the European Union's Horizon 2020 research and innovation program under grant agreement No 945063.

Data availability

The authors do not have permission to share data.

References

Sanchez-Espinoza, V.H., et al., 2021. The H2020 McSAFER project: main goals, technical work program, and status. Energies 14 (19), 6348.
Mercatali, L., Huaccho, G., Sanchez-Espinoza, V.-H., 2023. Multiphysics modeling of a reactivity insertion transient at different fidelity levels in support to the safety assessment of a SMART-like small modular reactor. Front. Energy Res. 11.
Ikonen, T., et al., 2016. Multiphysics simulation of fast transients with the FINIX fuel behaviour module EPJ Nuclear. Sci. Technol. 2 (37).
Xu, X., et al., 2022. Neutronics/thermal-hydraulics/fuel-performance coupling for light water reactors and its application to accident tolerant fuel. Ann. Nucl. Energy 166 (108809).
Zahur, A., Ali, M.R., Lee, D., 2023. Effect of two way thermal hydraulic-fuel performance coupling on multicycle depletion. Nucl. Eng. Technol. 55, 4431–4446.
Fridman, E., Bilodid, Y., Valtavirta, V., 2023. Definition of the neutronics benchmark of the NuScale-like core. Nucl. Eng. Technol. 55 (10), 3639–3647.
Molnar, B., Tolnai, G., Legrady, D., 2019. A GPU-based direct Monte Carlo simulation of time dependence in nuclear reactors. Ann. Nucl. Energy 132, 46–63.
Leppänen, J., et al., 2015. The Serpent Monte Carlo code: status, development and applications in 2013. Ann. Nucl. Energy 82, 142–150.
Imke, U., Sanchez-Espinoza, V.H., 2012. Validation of the subchannel code SUBCHANFLOW using the NUPEC PWR tests (PSBT). Sci. Technol. Nucl. Instal. 13.
Lassmann, K., 1992. TRANSURANUS: a fuel rod analysis code ready for use. 188, 295–302.
Van Uffelen, et al., Verification of the TRANSURANUS fuel performance code - an overview. In: 7th Int.Conf.on WWER Fuel Performance - Modelling and Experimental Support. 2007, INRNE: Albena, Bulgaria. p. 305-320.
Sanchez-Espinoza, V.H., et al., 2021. The McSAFE Project - High performance Monte Carlo based methods for safety demonstration: from proof of concept to industry applications. EPJ Web Conf., 247, 06004.
García, M., et al., 2020. A Serpent2-SUBCHANFLOW-TRANSURANUS coupling for pin-by-pin depletion calculations in Light Water Reactors. Ann. Nucl. Energy 139, 107213.
García, M., et al., 2021. Validation of Serpent-SUBCHANFLOW-TRANSURANUS pin-by-pin burnup calculations using experimental data from a Pre-Konvoi PWR reactor. Nucl. Eng. Des. 379, 111173.
Chen, S., Yuan, C., 2017. Neutronic analysis on potential accident tolerant fuel-cladding combination U3Si2-FeCrAl. Sci. Technol. Nucl. Install. 2017, 1–12.
Zhang, Z., et al., 2021. Core design and neutronic study on small reactor with advanced fuel designs. Nucl. Mater. Energy 29, 101068.
US NRC, 2022. NRC to Issue Rule Certifying NuScale Small Modular Reactor. US NRC, Office of Public Affairs: Washington, DC.
L.L.C. NuScale Power, 2020. NuScale Standard Plant Design Certification Application, Chapter Four, Reactor.
Salome Platform: open source integration platform for numerical simulation 2018; Available from: http://www.salome-platform.org/.
MED Module Documentation. CEA, EDF, OPENCASCADE 2018; Available from: https://docs.salome-platform.org/latest/dev/MEDCoupling/developer/index.html.
Deville, E., Perdu, F., 2021. Documentation of the Interface for Code Coupling. ICOCO, Paris.
Frazer, D., et al., 2021. High temperature mechanical properties of fluorite crystal structured materials (CeO2, ThO2, and UO2) and advanced accident tolerant fuels (U3Si2, UN, and UB2). J. Nucl. Mater. 554, 153035.
White, J.T., et al., 2015. Thermophysical properties of U_3Si_2 to 1773K. J. Nucl. Mater. 464, 275–280.
Yingling, J.A., et al., 2021. Updated U_3Si_2 thermal creep model and sensitivity analysis of the U_3Si_2-SiC accident tolerant fuel. J. Nucl. Mater. 543, 152586.
Liu, S., Liu, R., Qiu, C., 2023. Transient fuel behavior analysis of U3Si2 fuel and FeCrAl cladding based on multiphysics method. Prog. Nucl. Energy 159, 104648.
Gong, L., et al., 2013. Thermal conductivity of highly porous mullite materials. Int. J. Heat Mass Transf. 67, 253–259.

Pavlov, T.R., et al., 2021. Understanding the local thermal conductivity evolution of neutron irradiated U3Si2 dispersion fuel via state-of-the-art thermo-reflectance measurements. J. Nucl. Mater. 557, 153280.
Zhang, Y., Andersson, A.D.R., 2017. A thermal conductivity model for U-Si compounds, LANL.
Ulrich, T.L., et al., 2020. High temperature neutron diffraction investigation of U_3Si_2. Materialia 9, 100580.
Obbard, E.G., et al., 2018. Anisotropy in the thermal expansion of uranium silicide measured by neutron diffraction. J. Nucl. Mater. 508, 516–520.
Mannan, S., et al., 2003. Selection of materials for prototype fast breeder reactor. Trans. Indian Inst. Met. 56.
Cherubini, M., 2019. Implementation of preliminary FeCrAl properties in TRANSURANUS for the ACTOF Benchmark of the IAEA. In: International Workshop "Towards nuclear fuel modelling in the various reactor types across Europe", JRC, Editor. Karlsruhe, Germany.
Van Uffelen, P., Schubert, A., Soti, Z., 2023. Assessing the Effect of Some ATF Materials and Uncertainties on Their Properties Under Normal Operation Conditions by Means of the Transuranus Code. In: The 23rd Pacific Basin Nuclear Conference, Volume 3. Singapore: Springer Nature Singapore.
Chanaron, B., 2017. Overview of the NURESAFE European Project. Nucl. Eng. Des. 321, 1–7.
Chauliac, C., et al., 2011. NURESIM – A European simulation platform for nuclear reactor safety: multi-scale and multi-physics calculations, sensitivity and uncertainty analysis. Nucl. Eng. Des. 241 (9), 3416–3426.
Valtavirta, V., et al., 2021. Specifications for the Reactivity Transients Scenarios in the Four SMR Cores, McSAFER, Deliverable NUmber 3.1, in CORDIS, Helsinki, Finland.